Research Article

Tao Liu*, Lirui Mao, Facun Jiao, Chengli Wu, Mingdong Zheng, and Hanxu Li

Catalytic performance of Na/Ca-based fluxes for coal char gasification

https://doi.org/10.1515/gps-2022-0020
received October 07, 2021; accepted January 15, 2022

Abstract: Flux, able to improve the ash fusibility, usually contains catalytic metal compounds. Unfortunately, the quantitative analysis of synergistic catalysis effects between different fluxing agents on coal gasification has not been investigated thoroughly. In this study, the effect of the kinds and content of Na/Ca-based fluxes on char gasification was investigated in thermogravimetry analyzer (TGA). The synergistic catalysis effects and mechanism between the two kinds of fluxes were also studied. Finally, based on the TGA tests, the kinetics models for char gasification with flux addition were developed. The results showed that all the four Na-based fluxes could increase the char reactivity. Na_2CO_3, which afforded the best activity, could increase the reactivity by 5.3 times when the content was 5%. The five Ca-based fluxes had a weaker catalysis effect compared with Na-based fluxes. $CaCl_2$, exhibiting the best activity among the five Ca-based fluxes, could increase the reactivity by 2.3 times when the content was 5%. For composite fluxes, Na_2CO_3–CaO and Na_2CO_3–$CaCO_3$ had a remarkable synergistic effect, whereas others had less effect. Na_2CO_3 could inhibit the aggregation of Ca, which might cause the synergistic effects between Na and Ca fluxes. The random pore model was more suitable to describe the catalytic gasification process.

Keywords: coal gasification, flux, catalysis, synergistic effects, kinetics model

*** Corresponding author: Tao Liu,** School of Chemical Engineering, Anhui University of Science and Technology, Huainan 232001, China, e-mail: ltao_08@126.com
Lirui Mao, Facun Jiao, Chengli Wu: School of Chemical Engineering, Anhui University of Science and Technology, Huainan 232001, China
Mingdong Zheng, Hanxu Li: School of Chemical Engineering, Anhui University of Science and Technology, Huainan 232001, China; Institute of Energy, Hefei Comprehensive National Science Center, Hefei 230031, China

1 Introduction

Coal leads a dominant position in the energy consumption structure of China, and this situation is hard to change in a short period of time [1–3]. Coal gasification, the core of the clean and efficient utilization of coal, is the important process unit of technology such as integrated gasification combined cycle system, coal-derived chemicals production, and fuel cell [4,5]. It is also one of the key technologies of the clean energy industry due to its high thermal efficiency and near zero emission [6].

Entrained flow bed, which embodies many features such as elevated operation temperature, high operation pressure, and sufficient material mixing, is the mainstream of the development of coal gasification [7,8]. Theoretically, entrained flow bed can apply to nearly all types of coal [9]. However, this technology has certain requirements on the coal due to the problems of engineering. Ash fusibility is one of the engineering problems needing major consideration [10]. The ash fusion temperature (AFT) of the coal for coal-water slurry and pulverized coal gasifier is typically less than 1,400°C owing to the slag-tapping of the gasifier, and coal with high AFT can hardly meet this requirement [6,11]. However, the average ash content of coal in China is high (about 27–28%), and the reserves of coal with AFT higher than 1,400°C account for 57% of the China coal retained reserve [12,13]. Therefore, resolving the problem of the gasification of high AFT is of great value to make comprehensive use of the coal and adjust energy structure.

Flux can improve the ash fusibility remarkably [14–16]. Küçükbayrak et al. [17] concluded that acidic oxides such as Al_2O_3 and SiO_2 could form polymer in elevated temperature, which could increase the fusion temperature. The basic oxide could inhibit the formation of polymer, which could decrease the AFT [18]. Ca-based flux is the commonly used flux because of its remarkable ability to decrease the AFT and its low cost. Dai et al. [19] found that AFT decreased and then increased with the CaO content. CaO can not only decrease the AFT but also improve the viscosity-temperature characteristics. MgO can also decrease the AFT

significantly because Mg formed solid composites with Si, Fe, Ca, Mg, and Al [20]. Several studies showed that there was a synergistic effect between different fluxes. Wu et al. [15] found that MgO and CaO could decrease the AFT, and AFT decreased with MgO or CaO content. In addition, a synergistic effect of MgO and CaO was observed. Zhang et al. [16] also confirmed the synergistic effect between CaO and MgO.

Most fluxing agents contain alkali metal and alkaline-earth metal elements that could also catalyze coal gasification. Na-based and Ca-based compounds are the typical catalysts been studied. Their catalytic mechanisms have been widely discussed [21–23]. Synergistic effects of catalysts containing different elements have also been investigated [23–26]. Gao et al. [25] conducted experiments to investigate the effect of Na/Ca compounds (calcium acetate and sodium acetate as precursors) on coal gasification performance and coal char characteristics. The results showed a combined effect toward the gasification reactivity, and Na compounds could inhibit the agglomeration of CaO. Mei et al. [24] found that Ca additive could inhibit the reaction between Na and Si, Al minerals, and, therefore, Na is kept active during catalytic gasification. Bai et al. [26] also found that Ca coexist with Na has a better catalytic effect compared to Na and Ca alone.

Although synergistic effects between Na and Ca compounds on coal gasification were studied, the quantitative analysis of synergistic effects between different Na and Ca compounds on coal gasification has not been investigated thoroughly. In this study, typical Na-based and Ca-based flux agents were selected. The effect of the kinds and content of flux on coal char gasification was investigated. The synergistic catalysis effects between Na-based and Ca-based flux were also analyzed quantitatively. Finally, based on the TGA tests and kinetics analysis, kinetics models for coal char gasification with flux addition were developed. The results should be helpful for the design of flux with fine catalytic effect on coal gasification.

2 Experimental

2.1 Materials

In this study, typical Huainan coal (ZJX) having high AFT was selected. According to the national standard GB/T19494-2-2004, the selected coal sample was dried in air, crushed, sieved, and ground to below 74 μm. The proximate and ultimate analysis of coal samples were conducted according to the national standards GB/T212-2008 and GB/T476-2001, respectively. The results of the proximate and ultimate analysis are shown in Table 1.

The preparation of the coal char sample used in the thermogravimetric experiment was conducted as follows: (1) to eliminate the influence of ash on the coal char gasification, acid deashing was performed to remove the ash from the coal, and the detailed procedure is shown in Figure A1 (in Appendix) (2) The deashed coal was then put in a tube furnace (a schematic of the device is shown in Figure 1, where it was heated from room temperature to 900°C in a nitrogen (99.999%) atmosphere at a heating rate of 10°C·min^{-1}, and the final temperature was held for 1 h. Devolatilization under this condition could ensure eliminating the impact of volatility and moisture in the coal. The proximate and ultimate analysis of demineralized coal char are shown in Table 1. (3) The flux (Na_2CO_3, $CaCO_3$, CaO, NaCl, $CaCl_2$, Na_2SO_4, $CaSO_4$, Na_2SiO_3, or $CaSiO_3$) with mass fractions of 1, 2, 5, and 10% was added to the deashed coal char. The soluble additives (Na_2CO_3, NaCl, $CaCl_2$, Na_2SO_4, and Na_2SiO_3) were loaded by isometric solution impregnation method, and the insoluble components ($CaCO_3$, CaO, $CaSO_4$, and $CaSiO_3$) were loaded by mechanical stirring method. The composite flux was added according to its water solubility; that is, the water-soluble flux was first loaded by solution impregnation method, and the insoluble flux was loaded by mechanical stirring method after drying. After the flux loading, the samples were dried at 105°C for 12 h. To verify the accuracy of the concentrations of flux in prepared samples, the concentrations in partial

Table 1: Proximate and ultimate analysis of ZJX coal and ash-free ZJX coal char

Sample	Proximate analysis (wt%)				Ultimate analysis (wt%)				
	M_{ad}	A_{ad}	V_{ad}	FC_{ad}	C_{ad}	H_{ad}	N_{ad}	O_{ad}*	S_{ad}
ZJX	2.03	20.98	28.17	48.82	63.81	4.18	1.18	7.51	0.31
Ash-free char	0.25	0.51	0.79	98.45	93.38	1.78	1.24	2.55	0.29

*Calculated by difference.

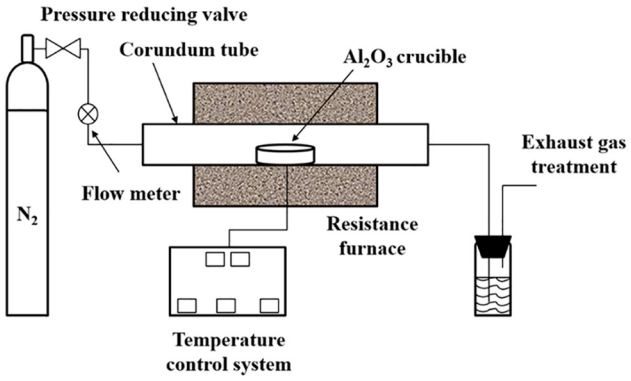

Figure 1: Schematic of coal char preparation system.

samples (shown in Table A1 in Appendix) were detected by digestion combined with inductively coupled plasma optical emission spectrometry. The details of the digestion are shown in an earlier study [27], and the accuracy was controlled within ±5%. The source and grade of chemicals in this study are shown in Table 2.

2.2 Method and apparatus

The CO_2 gasification reactivity of coal char was determined using a NETZSCH (Germany) STA 449 F3 thermogravimetric analyzer. A preliminary experiment was conducted before the actual experiment to select the optimal particle size, gas flow rate, and sample quality to eliminate the influence of internal and external diffusion on the reaction. The experimental process was as follows: a certain mass of sample was weighed into a corundum crucible. The sample was heated to the target temperature at a heating rate of 20°C·min^{-1} in a nitrogen atmosphere, the gas was then switched to CO_2, and the sample was kept warm for 90 min.

The carbon conversion rate was calculated according to the following equation:

$$X = \frac{m_0 - m_t}{m_0 - m_{\text{end}}} \tag{1}$$

where X is the carbon conversion rate (%), m_0 is the initial mass of coal char (mg), m_t is the mass of coal char at the reaction time t (mg), and m_{end} is the mass of coal char after the reaction (mg).

To quantify the gasification reaction activity of coal char with different flux addition, the gasification reactivity index ($R_{0.5}$) was introduced. High $R_{0.5}$ values indicate a high coal gasification reaction activity. The $R_{0.5}$ value can be calculated as follows [28]:

$$R_{0.5} = \frac{0.5}{\tau_{0.5}} \tag{2}$$

where $R_{0.5}$ is expressed in min^{-1} and $\tau_{0.5}$ is the gasification time required to reach 50% of carbon conversion rate (min).

In this study, the $R_{0.5}$ values were in the range 0.005–0.040. To facilitate data processing and comparison, the obtained $R_{0.5}$ values were multiplied by 10^3. In addition, all the tests were repeated three times, and the reported gasification indexes were average values. The relative error is less than 5%.

The distribution of Na and Ca elements was analyzed by a TESCAN (China) VEGA3 scanning electron microscope (SEM) coupled with a BRUKER (Germany) energy dispersive spectrometer.

2.3 Kinetic model

Different kinetic models such as random pore model (RPM), homogeneous model (HM), unification theory model, and shrinking core model (SCM) can be applied for investigating the kinetics of coal gasification [29–32].

Table 2: Reagent specifications and manufacturers

Reagents	Reagent specifications	Manufacturers
Hydrochloric acid (37%)	AR	Sinopharm Chemical Reagent Limited Corporation
Hydrofluoric acid (47%)	AR	Sinopharm Chemical Reagent Limited corporation
Na_2CO_3	AR	Aladdin
$CaCO_3$	AR	Sinopharm Chemical Reagent Limited Corporation
CaO	AR	Sinopharm Chemical Reagent Limited Corporation
NaCl	AR	Sinopharm Chemical Reagent Limited Corporation
$CaCl_2$	AR	Sinopharm Chemical Reagent Limited Corporation
Na_2SO_4	AR	Sinopharm Chemical Reagent Limited Corporation
$CaSO_4$	AR	Aladdin
Na_2SiO_3	AR	Aladdin
$CaSiO_3$	AR	Sinopharm Chemical Reagent Limited Corporation

To find the model that best fits the coal gasification process, HM, RPM, and SCM were selected based on earlier studies to fit the gasification reaction data.

2.3.1 HM [30]

The HM is the simplest and most commonly used coal gasification model. This model only considers the relationship between the conversion rate and the gasification time and not the influence of the gas–solid reaction surface area and active sites on the carbon conversion rate during the reaction process. HM assumes that the internal and external diffusion is so fast that its influence can be eliminated, and that the entire reaction process occurs inside. The coal particles maintain the same size during the gasification process, but the density changes uniformly. The integral rate expression is as follows [33,34]:

$$\mathrm{d}x/\mathrm{d}t = k_{\mathrm{HM}}(1 - x) \tag{3}$$

where x is the carbon conversion rate, k is the gasification reaction rate constant (s^{-1}), and t is the gasification reaction time (s).

2.3.2 RPM

RPM assumes that the coal char particles have a large number of cylinders with different pore diameters. The gas reactant reacts with the inner wall of the cylindrical hole of the coal char particles, and the connected pores are cross-linked during the reaction. All the products from the reaction process precipitate in the form of gas. The RPM ignores the influence of gas diffusion and is represented by the following expression [33]:

$$\mathrm{d}x/\mathrm{d}t = k_{\mathrm{RPM}}(1 - x)[\sqrt{1 - \varphi \ln(1 - x)} - 1] \tag{4}$$

where x is the carbon conversion rate, k is the gasification reaction rate constant (s^{-1}), φ is the sample particle structure parameter, and t is the gasification reaction time (s).

$$\varphi = \frac{4\pi L_0(1 - \varepsilon_0)}{S_0^2} \tag{5}$$

where S_0, L_0, and ε_0 are the specific surface area in the initial reaction, the total volume pore length, and the initial porosity of the sample, respectively.

2.3.3 SCM

The SCM assumes that the gas–solid two-phase reaction only occurs on the outer surface of the solid particle. As the reaction proceeds, the reaction surface gradually migrates from the outside to the inside of the particle, and the size of the unreacted core gradually decreases until its complete disappearance. When the gasification process is controlled by the chemical reaction, the reaction formula of the SCM is as follows [35]:

$$\mathrm{d}x/\mathrm{d}t = k_{\mathrm{SCM}}(1 - x)^{2/3} \tag{6}$$

where x is the carbon conversion rate, k is the gasification reaction rate constant (s^{-1}), and t is the gasification reaction time (s).

3 Results and discussion

3.1 Influence of Na-based flux on the reactivity of coal char gasification

To investigate the influence of different Na-based fluxes on the coal char gasification characteristics, the deashed coal char was loaded with 5% Na_2CO_3, NaCl, Na_2SO_4, and Na_2SiO_3, and an isothermal CO_2 gasification experiment was performed at 1,000°C. The experimental results are shown in Figure 2, from which it can be extracted that the addition of Na-based flux can significantly improve the gasification reaction activity. Figure 2a shows that under a gasification time of 30 min, the carbon conversion rate was the lowest (20%) for deashed coal char without flux and the highest (95%) after adding Na_2CO_3. Meanwhile, the addition of Na_2SO_4, NaCl, and Na_2SiO_3 afforded a carbon conversion rate of 91%, 69%, and 56%, respectively. Therefore, the activity of the four Na-based fluxes followed the order: Na_2CO_3 > Na_2SO_4 > NaCl > Na_2SiO_3.

According to Figure 2, $R_{0.5}$ increased with the addition of the Na-based flux components from the lowest value of only 5.89 for the deashed coal char to 37.32 after loading Na_2CO_3, which represents an increase of 5.3 times, 36.09 after loading Na_2SO_4 (5.1 times increase), 24.05 after loading NaCl (3.1 times increase), and 19.17 with Na_2SiO_3 (2.3 times increase). These results confirm the trend for the catalytic activity obtained from the results of the carbon conversion rate.

Figure 3 shows the influence of the Na-based flux content on $R_{0.5}$. As shown in Figure 3a, $R_{0.5}$ initially increased with increasing the Na_2CO_3 loading capacity up to 5%, reaching the maximum value of 37.2, which is 5.9 times higher than that obtained in the absence of flux. Then, upon further increasing the Na_2CO_3 content, $R_{0.5}$ showed a downward trend. This suggests that the catalytic ability of Na_2CO_3 is not always proportional to

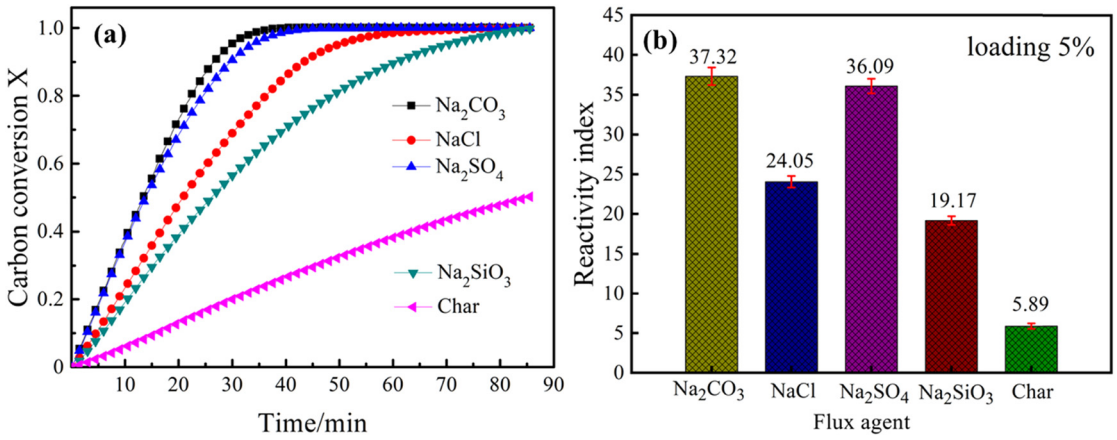

Figure 2: Effect of Na-based flux agents on the reactivity of ZJX char: (a) gasification rate and (b) gasification reactivity index.

the loading capacity and exhibits a saturation point above which the catalytic ability decreases. As shown in Figure 3b, increasing the NaCl amount from 1% to 2% did not increase the $R_{0.5}$ value significantly. In contrast, the addition of NaCl up to 5% caused a sharp increase of $R_{0.5}$ to 24.05, which is 3.1 times higher than that of the sample without NaCl. Figure 3c displays the relationship between the Na_2SO_4 content and $R_{0.5}$. When the Na_2SO_4 loading capacity was 1%, 2%, and 5%, $R_{0.5}$ was 11.62, 17.30, and 36.09, respectively, which are 1.9, 2.9, and 5.1 times higher than the values obtained without flux addition. The relationship between the Na_2SiO_3 loading capacity and $R_{0.5}$ is shown in Figure 3d, which reveals that $R_{0.5}$ increased smoothly with the increase of the Na_2SiO_3 loading

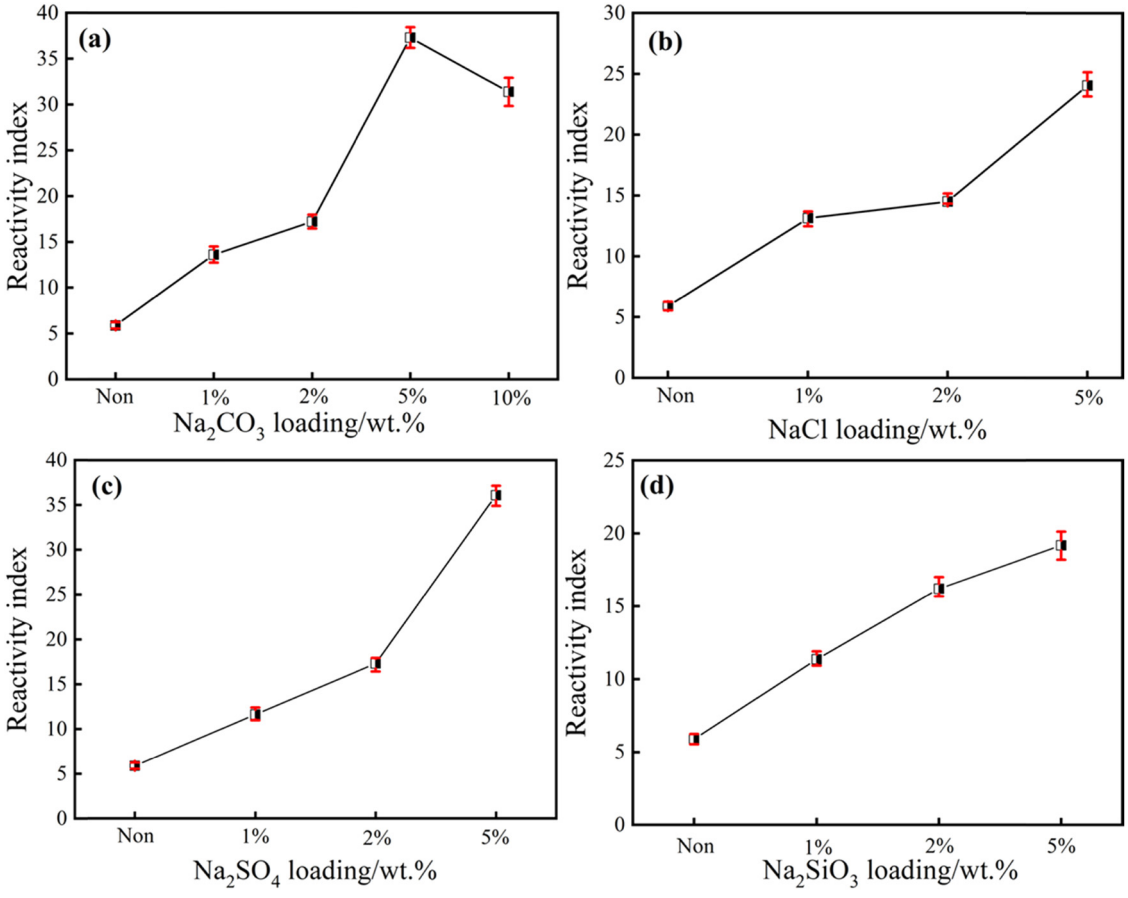

Figure 3: Effect of Na-based flux agent content on the reactivity index of ZJX char: (a) Na_2CO_3, (b) NaCl, (c) Na_2SO_4 and (d) Na_2SiO_3.

capacity. Thus, under a loading capacity of 1%, 2%, and 5%, $R_{0.5}$ was 11.36, 16.20, and 19.17, respectively, which represents an increase of 0.9, 1.8, and 2.3 times compared with the values obtained without catalyst addition. In summary, the 5% Na_2CO_3 flux afforded the highest coal char reactivity. Mei et al. [24] also found that Na_2CO_3 had the best catalytic effect on coal gasification compared to other Na-based compound such as $NaAlO_2$ and sodium aluminum silicate.

3.2 Influence of Ca-based flux on the coal char gasification reactivity

To investigate the influence of the Ca-based flux on the coal char gasification characteristics, deashed coal char was loaded with 5% CaO, $CaCO_3$, $CaCl_2$, $CaSiO_3$, and $CaSO_4$, and an isothermal CO_2 gasification experiment was conducted at 1,000°C. As shown in Figure 4, $CaCl_2$ and $CaSO_4$ had the best and the worst catalytic effect, respectively, and CaO, $CaCO_3$, and $CaSiO_3$ exhibited similar catalytic ability between that of $CaCl_2$ and $CaSO_4$. Overall, the Ca-based flux showed weaker catalytic ability than the Na-based flux. According to these results, the activity of the selected Ca-based fluxes followed the order: $CaCl_2$ > CaO ≈ $CaCO_3$ ≈ $CaSiO_3$ > $CaSO_4$.

The influence of the Ca-based flux on $R_{0.5}$ is shown in Figure 4b. The $R_{0.5}$ value of the sample with $CaCl_2$ was 19.17, which is 2.3 times higher than that obtained without flux, and the reaction activity was the highest. The samples loaded with CaO, $CaCO_3$, and $CaSiO_3$ exhibited similar $R_{0.5}$ values of 12.73, 13.61, and 12.81, respectively, which indicates that these three fluxes had similar catalytic ability. The $R_{0.5}$ of the sample loaded with $CaSO_4$ was 6.71, which is only 0.82 higher than that of the sample without catalyst, indicating an extremely weak catalytic capacity. Again, the $R_{0.5}$ value and the carbon conversion rate followed a consistent trend.

Figure 5 shows the influence of the Ca-based flux loading capacity on the $R_{0.5}$ of coal char. $R_{0.5}$ increased from 5.89 to 12.50, which represents an increase of 1.1 times, with the increase of the CaO loading capacity up to 2%. Above this point, the increasing trend weakened. The observed weak catalytic effect of CaO may be related to the loading method. Some studies have shown that CaO loaded via the solution impregnation method has a better catalytic effect than that loaded using the mechanical mixing method. In the former method, CaO reacts with deionized water to form a $Ca(OH)_2$ emulsion; therefore, part of the Ca exists in the form of ions, which are easier to disperse evenly on the coal surface [36]. Murakami et al. [21] demonstrated that the activity of $CaCO_3$ was as high as catalyst using an solution impregnation method such as $Ca(OH)_2$ aqueous. This might be due to using steam as the gasification agent.

As shown in Figure 5b, the catalytic ability of $CaCO_3$ was similar to that of CaO. $R_{0.5}$ increased first and then decreased with the increase of $CaCO_3$, reaching its maximum value at 5%. At this point, the reactivity index was determined to be 13.61, which is 1.3 times higher than that of the sample without flux. Upon further increasing the $CaCO_3$ amount, the catalytic ability was reduced. This is consistent with the results reported by Yu et al. [37], according to which an excess of catalyst would block the coal char gaps, affecting the transfer of the gasification agent. Figure 5c shows that $R_{0.5}$ also increased gradually with the increase of the $CaCl_2$ amount. This increase was relatively rapid below an amount of 2%, at which the $R_{0.5}$ value was 17.14 (1.9 times higher than

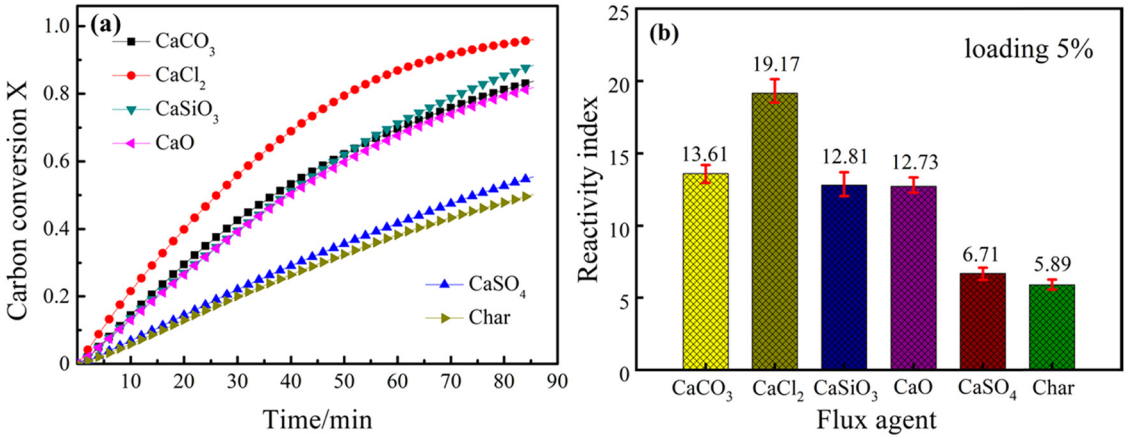

Figure 4: Effect of Ca-based flux agents on the reactivity of ZJX char: (a) gasification rate and (b) gasification reactivity index.

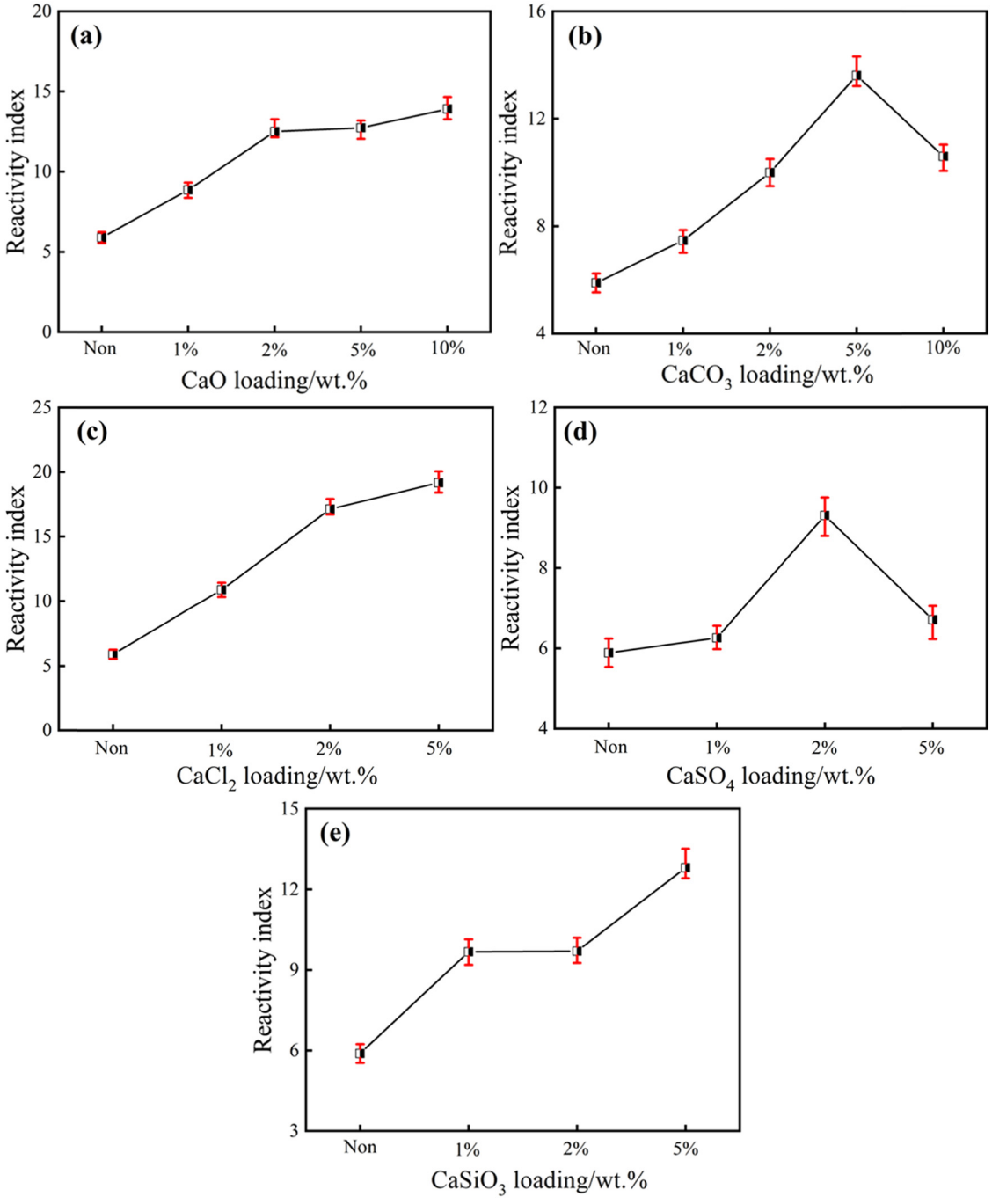

Figure 5: Effect of Ca-based flux agent content on the reactivity index of ZJX char: (a) CaO, (b) $CaCO_3$, (c) $CaCl_2$, (d) $CaSO_4$ and (e) $CaSiO_3$.

that of the sample without catalyst). Above 2% of $CaCl_2$ amount, $R_{0.5}$ increased more slowly, reaching 19.17 (2.3 times higher than that in the absence of catalyst) at an amount of 5%. Figure 5d reveals the poor catalytic effect of $CaSO_4$. No significant change in $R_{0.5}$ compared with the sample without catalyst was observed when adding 1% and 5% $CaSO_4$, and an amount of 2% afforded a slight increase in $R_{0.5}$ (9.31, 0.6 times increase). As can be extracted from Figure 5e, when the $CaSiO_3$ loading capacity was 1%, 2%, and 5%, the $R_{0.5}$ value was 9.68, 9.70, and 12.81, respectively. With the increase of $CaSiO_3$, $R_{0.5}$ first increased and then remained almost constant, to finally increase again. The addition of 1% $CaSiO_3$ enhanced the coal char gasification activity significantly, which was basically unchanged from 1% to 2%, and then improved again for 5% $CaSiO_3$.

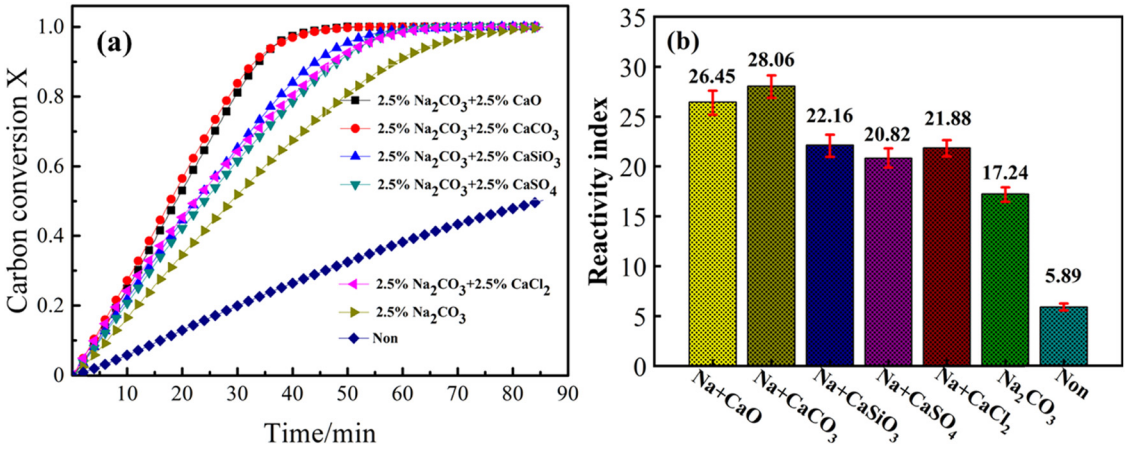

Figure 6: Effect of Na/Ca composite flux agent on the reactivity of ZJX char: (a) gasification rate and (b) gasification reactivity index.

3.3 Influence of Na/Ca composite flux on the coal char gasification reactivity

To study the synergy between the Na and Ca fluxes, Na_2CO_3, which had the best effect among the single-component fluxes, was combined with other Ca-based catalysts for catalytic gasification. A CO_2 gasification experiment was performed at 1,000°C using the following samples: 2.5% Na_2CO_3/2.5% CaO, 2.5% Na_2CO_3/2.5% $CaCO_3$, 2.5% Na_2CO_3/2.5% $CaSiO_3$, 2.5% Na_2CO_3/2.5% $CaSO_4$, 2.5% Na_2CO_3/2.5% $CaCl_2$, and 2% Na_2CO_3. The experimental results are depicted in Figure 6. Figure 6a shows that the sample with the composite flux was the first to be gasified completely within 60 min, followed by the sample loaded with Na_2CO_3 alone, which took 75 min to be gasified. For the sample without flux, the carbon conversion rate was only 50% after 85 min of reaction.

Figure 6b shows the effect of the Na/Ca synergistic catalysis effect on $R_{0.5}$. The sample without flux had the lowest $R_{0.5}$, followed by the sample with Na_2CO_3 alone. The Na/Ca composite flux afforded a higher $R_{0.5}$ value than that obtained with Na_2CO_3 alone and without catalyst, indicating its higher activity. The sample containing Na_2CO_3/$CaCO_3$ exhibited the highest $R_{0.5}$ of 28.06, which is 3.8 times higher than that of the sample without catalyst and 0.6 times higher than that obtained with single Na_2CO_3. The sample with Na_2CO_3/CaO afforded an $R_{0.5}$ of 26.45, which is 3.5 times higher than that of the sample without catalyst and 0.5 times higher than that with single Na_2CO_3. The samples containing Na_2CO_3/$CaSiO_3$, Na_2CO_3/$CaSO_4$, and Na_2CO_3/$CaCl_2$ showed similar $R_{0.5}$ values of 20–22.5, which were about 2.5–2.8 times higher than that of the sample without catalyst and 0.2–0.3 times higher than that obtained with single Na_2CO_3.

To further explore the synergy between Na and Ca, the synergistic effects were quantified by calculating the theoretical reactivity index (R_{theory}) as follows:

$$R_{theory} = X_1R_{Na} + X_2R_{Ca} \quad (7)$$

where X_1 and X_2 are the ratio coefficients of Na and Ca in the composite additives, R_{Na} is the reactivity index when 5% Na additives are added, and R_{Ca} is the reactivity index when 5% Ca flux is added.

The as-calculated theoretical reactivity indexes were compared with the experimental values to confirm the existence of a synergistic effect between the Na/Ca catalysts, which occurs when the experimental value exceeds the theoretical value. The results are shown in Table 3.

Among the five compound additives, only 2.5% Na_2CO_3/2.5% CaO and 2.5% Na_2CO_3/2.5% $CaCO_3$ afforded experimental reactivity indexes greater than the theoretical values, which suggests the occurrence of synergistic effect only when Na_2CO_3 was compounded with CaO or $CaCO_3$. Moreover, the best synergistic effect was obtained with the combination of Na_2CO_3 and $CaCO_3$.

To investigate the influence of the ratio of the Na/Ca flux on the catalytic gasification of coal char, Na_2CO_3, and

Table 3: Comparison of actual reactivity index and theoretical reactivity index

Flux	R_{theory}	$R_{experimental}$
2.5% Na_2CO_3–2.5% CaO	25.02	26.45
2.5% Na_2CO_3–2.5% $CaCO_3$	25.46	28.06
2.5% Na_2CO_3–2.5% $CaSiO_3$	25.07	22.16
2.5% Na_2CO_3–2.5% $CaSO_4$	22.02	20.82
2.5% Na_2CO_3–2.5% $CaCl_2$	28.25	21.88

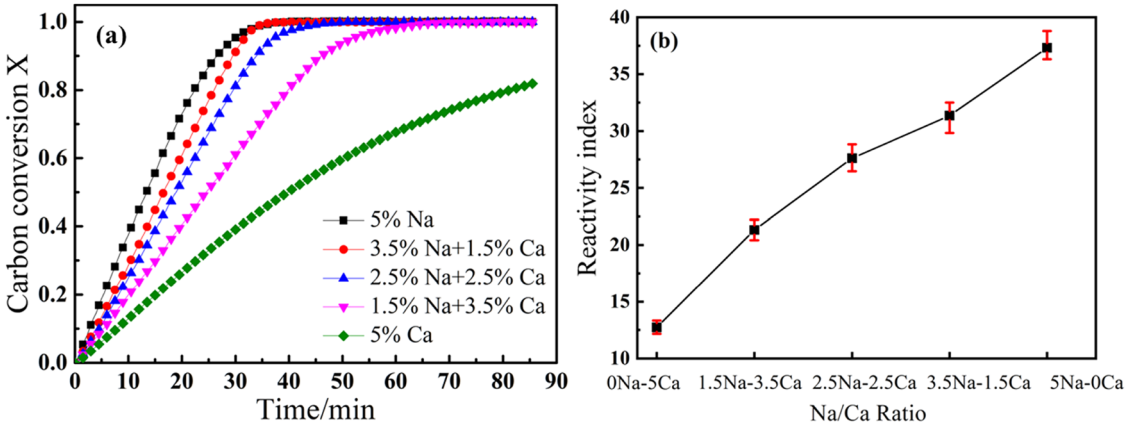

Figure 7: Effect of Na/Ca composite flux agent content on the reactivity of ZJX char: (a) gasification rate and (b) gasification reactivity index.

CaO were compounded in different proportions. Samples containing 1.5% Na_2CO_3/3.5% CaO, 2.5% Na_2CO_3/2.5% CaO, and 3.5% Na_2CO_3/1.5% CaO were compared in a CO_2 gasification experiment at 1,000°C with those having exclusively Na_2CO_3 or CaO. The experimental results are shown in Figure 7. Among the Na/Ca composite fluxes, the sample with the highest Na_2CO_3 content afforded the best catalytic effect. Figure 7b shows the effect of the Na/Ca ratio on $R_{0.5}$. The carbon conversion rate increased with the Na/Ca ratio. The sample with 1.5% Na_2CO_3/3.5% CaO exhibited significantly higher gasification activity than the sample with CaO alone, and the gasification reaction index increased by 0.67 times. The gasification reaction index of the samples with 2.5% Na_2CO_3/2.5% CaO and 3.5% Na_2CO_3/1.5% CaO increased by 1.17 and 1.46 times, respectively, compared with that of the sample with CaO alone.

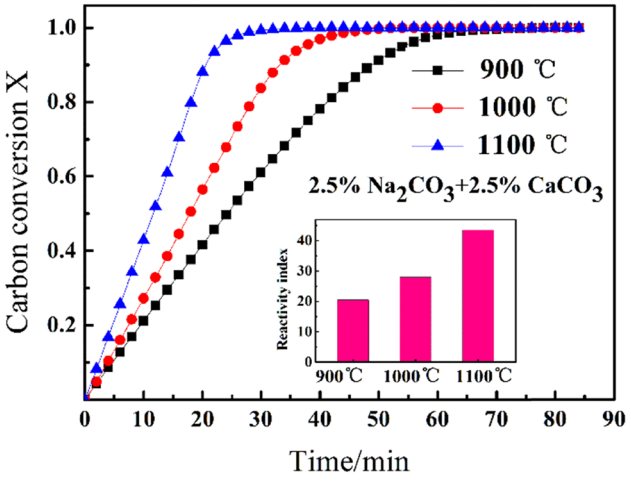

Figure 8: Effect of gasification temperature on the reactivity index and carbon conversion rate of ZJX char with composite flux agent addition.

Figure 8 shows the gasification reaction of the sample with 2.5% Na_2CO_3/2.5% $CaCO_3$ at three different temperatures, that is, 900°C, 1,000°C, and 1,100°C. The gasification activity was found to increase significantly with the temperature. Thus, the reaction required 60 min to reach completion at 900°C, 40 min at 1,000°C, and only 25 min at 1,100°C. Similarly, $R_{0.5}$ increased with the gasification temperature, being 0.40 and 1.12 times higher at 1,000°C and 1,100°C, respectively, than at 900°C.

To investigate the mechanism of synergistic catalysis effects, the Na and Ca elemental mapping of char residues after TGA tests under 1,000°C were collected on SEM-EDX. As shown in Figure 9a and b, Na exhibited better dispersity, whereas Ca showed aggregation to some extent. This might be the reason for the better catalysis effect of Na_2CO_3. As shown in Figure 9c, Na_2CO_3 could inhibit the aggregation of Ca and increase the dispersity of Ca, which might cause the synergistic catalysis effects between Na_2CO_3 and $CaCO_3$. Gao et al. [25] also found that Na-based catalyst could inhibit the agglomeration of CaO due to its fine mobility and the formation of Na–Ca compound.

3.4 Kinetics of char gasification with flux addition

The kinetics of the gasification reaction of the sample with 2.5% Na_2CO_3/2.5% $CaCO_3$ were investigated at 900°C, 1,000°C, and 1,100°C, and the most suitable kinetic model to describe the process in the presence of flux was determined.

The three models mentioned in Section 2.3 were used to fit the gasification reaction data, and the linear regression fitting curves of the samples at different

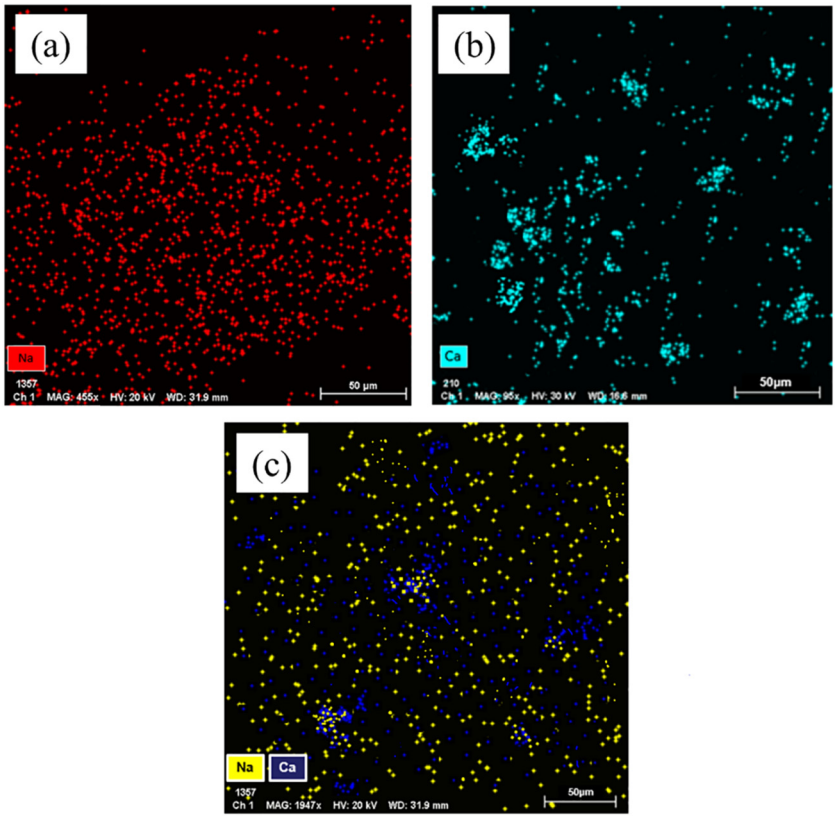

Figure 9: Na/Ca element mapping analysis of char residue of gasification: (a) residues of char with 5% Na_2CO_3 addition, (b) residues of char with 5% $CaCO_3$ addition, and (c) residues of char with 2.5% Na_2CO_3 and 2.5% $CaCO_3$ addition.

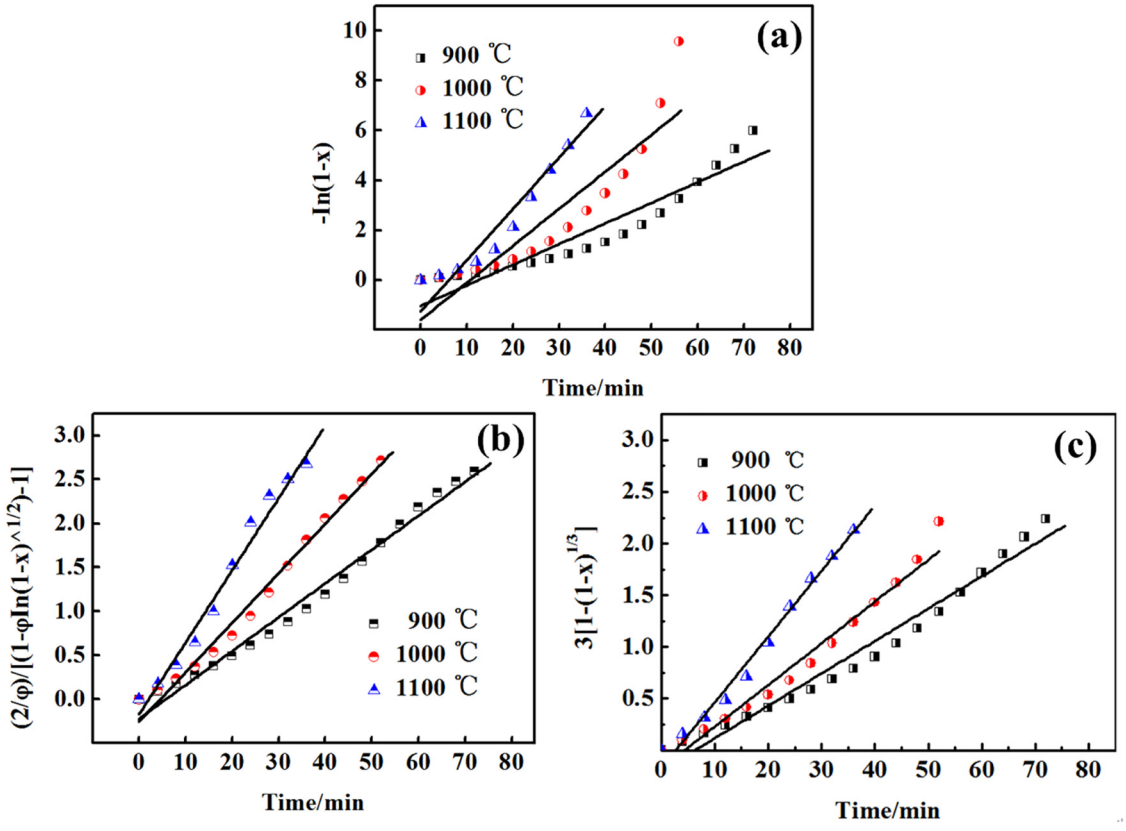

Figure 10: Fitting curve of carbon conversion using different kinetic models: (a) HM, (b) RPM, and (c) SCM.

Table 4: Fitting parameters of different kinetic models

T (°C)	HM		RPM		SCM	
	R	*K* (10^3·s^{-1})	*R*	*K* (10^3·s^{-1})	*R*	*K* (10^3·s^{-1})
900	0.9384	0.0827	0.9880	0.0314	0.9475	0.0385
1,000	0.8118	0.1484	0.9975	0.0403	0.9278	0.0564
1,100	0.8945	0.2058	0.9823	0.0634	0.9365	0.0821

temperatures were obtained as shown in Figure 10. Fitting parameters of different kinetic models are shown in Table 4.

It can be seen from the fitting data summarized in Table 4 that the fitting coefficients of the three models were all more than 0.8, indicating that to a certain extent, the three models can be applied to the coal catalytic gasification process. The SCM and the RPM afforded high fitting coefficients more than 0.97, indicating that these two models are more suitable to describe the process of coal catalytic gasification. As the HM does not consider the influence of surface area and active sites of the gas–solid reaction on the carbon conversion rate during the reaction, the corresponding fitting coefficient was relatively low.

The kinetic parameters were calculated using the Arrhenius formula:

$$k = Ae^{-\frac{E}{RT}} \tag{8}$$

where E is the apparent activation energy of the reaction (kJ·mol^{-1}), T is the reaction temperature (K), A is the pre-exponential factor (min^{-1}), and R is the gas reaction constant (8.314 J·mol^{-1}·K^{-1}).

By taking the logarithm on both sides of the Arrhenius formula, the following formula is obtained as follows:

$$\ln k = \ln A - \frac{E}{RT} \tag{9}$$

By calculating the thermogravimetric data at different temperatures and plotting $\ln k$ vs $1/T$, the A and E values can be determined from the intercept and the slope of the resulting straight line, respectively. The fitting results of the three models are shown in Figure 11. Similarly, the gasification experimental data of the samples without flux, with 5% Na_2CO_3, and with 5% $CaCO_3$ were fitted at 900°C, 1,000°C, 1,100°C to obtain the kinetic parameters. The results are shown in Table 5.

As can be extracted from Table 5, the fitting coefficient of the HM was low. In contrast with the fitting coefficient of the noncatalytic gasification, which was higher than 0.96, the fitting coefficients of the three catalytic gasification samples were lower than 0.94, the fitting coefficients of the RPM were all more than 0.98, and the fitting coefficients of the SCM were between 0.92

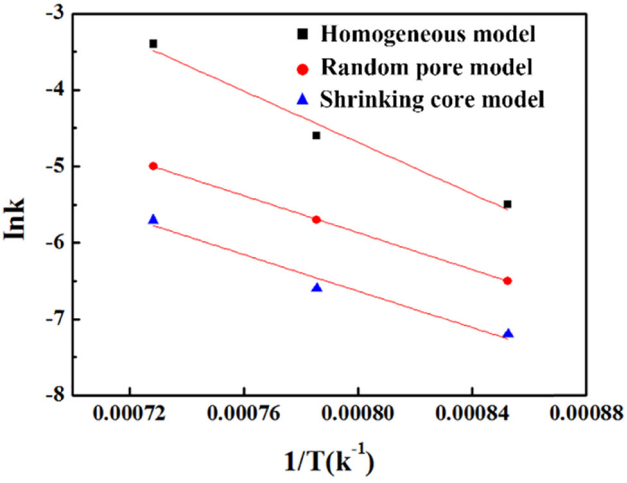

Figure 11: Fitting curves of the three kinetic models.

Table 5: Dynamic parameters corresponding to the three models

Samples	HM			RPM			SCM		
	ln *A*	*E* (kJ·mol^{-1})	*R*	ln *A*	*E* (kJ·mol^{-1})	*R*	ln *A*	*E* (kJ·mol^{-1})	*R*
Non	19.48	210.54	0.9673	24.59	236.34	0.9871	17.16	221.38	0.9658
5% Na_2CO_3	8.58	133.21	0.9314	11.64	159.87	0.9917	8.14	142.26	0.9544
5% $CaCO_3$	11.96	188.49	0.9286	13.30	198.47	0.9869	11.02	185.63	0.9717
2.5% Na_2CO_3–2.5% $CaCO_3$	9.13	139.96	0.9154	12.55	164.05	0.9952	8.86	148.39	0.9287

and 0.98. These results indicate that the RPM afforded the best fit and the HM the worst.

According to the activation energy data, the noncatalytic gasification exhibited high reaction activation energy. The activation energy calculated using the RPM was the highest, 236.34 kJ·mol^{-1}, and that obtained with the HM was the lowest, 210.54 kJ·mol^{-1}. After the catalyst addition, the activation energy of the gasification reaction was significantly reduced. When 5% Na_2CO_3, 5% $CaCO_3$, and 2.5% Na_2CO_3/2.5% $CaCO_3$ were added, the activation energy for the catalytic gasification calculated using the RPM decreased to 133.21, 188.49, and 139.96 kJ·mol^{-1}, respectively, which represents a reduction of 44%, 20%, and 41%. The reduction in activation energy followed the order: 5% Na_2CO_3 > 2.5% Na_2CO_3/2.5% $CaCO_3$ > 5% $CaCO_3$.

Coal char gasification experiments were carried out in thermogravimetry in this study. The gasification process in thermogravimetry is different from entrained flow bed especially in mass transfer and heat transfer. Different diffusion rates of flux can influence the synergistic catalysis effects between different fluxing agents, whereas the heat transfer rate also has impact on the gasification rate. To further investigate the effect of heat and mass transfer on synergistic catalysis effects, dropper furnace may be more applicable. In addition, cross-sectional analysis of residues in different retention time needs to be paid more attention.

4 Conclusion

The catalytic performance of Na/Ca-based flux for coal gasification was systematically studied in thermogravimetric analyzer. The synergistic catalysis effects between Na-based and Ca-based flux were also studied. Based on the TGA tests and kinetics analysis, kinetics model for coal char gasification with flux addition was developed. The main conclusions are as follows:

1. The four Na-based flux, Na_2CO_3, Na_2SO_4, NaCl, and Na_2SiO_3, could increase the reactivity of coal char, and the strength of catalysis effect order was Na_2CO_3 > Na_2SO_4 > NaCl > Na_2SiO_3.
2. Ca-based flux had weaker catalysis effect compared with Na-based flux, and the strength of catalysis effect order of Ca-based flux was $CaCl_2$ > CaO ≈ $CaCO_3$ ≈ $CaSiO_3$ > $CaSO_4$.
3. For composite flux, Na_2CO_3–CaO and Na_2CO_3–$CaCO_3$ had remarkable synergistic catalysis effect, whereas Na_2CO_3–$CaSiO_3$, Na_2CO_3–$CaCl_2$, and Na_2CO_3–$CaSO_4$ had no synergistic effect.
4. The RPM with the model function $dx/dt = k_{RPM}(1 - x)[\sqrt{1 - \varphi \ln(1 - x)} - 1]$ had better fitting effect for char gasification with flux addition.

Funding information: This research program was financially supported by Natural Science Research Project of Colleges and Universities in Anhui Province (no. KJ2021A0432), the Institute of Energy, Hefei Comprehensive National Science Center (no. 19KZS203), University-level key projects of Anhui University of science and technology (no. xjzd2020-07), the University Synergy Innovation Program of Anhui Province (no. GXXT-2020-006), and the Scientific Research Foundation for the Introduction of Talent, Anhui University of Science and Technology (no. 13190288).

Author contributions: Tao Liu: writing – original draft, writing – review and editing, methodology, formal analysis, and visualization; Lirui Mao: data curation, formal analysis, and resources; Facun Jiao: investigation and software; Chenli Wu: validation; Mingdong Zheng: funding acquisition, conceptualization, and supervision; and Hanxu Li: project administration, conceptualization, and supervision.

Conflict of interest: Authors state no conflict of interest.

Data availability statement: All data generated or analyzed during this study are included in this published article.

References

[1] Xu B, Cao Q, Kuang D, Gasem KAM, Adidharma H, Ding D, et al. Kinetics and mechanism of CO_2 gasification of coal catalyzed by Na_2CO_3, $FeCO_3$ and Na_2CO_3–$FeCO_3$. J Energy Inst. 2020;93(3):922–33.

[2] Liu T, Yu Z, Jiao F, Li H, Fang Y. Effect of preparation conditions on the performance of K-decorated Fe_2O_3/Al_2O_3 oxygen carrier (OC) in chemical looping conversion of coal process with deep OC reduction. J Energy Inst. 2021;98:179–87.

[3] Yu J, Guo Q, Ding L, Gong Y, Yu G. Studying effects of solid structure evolution on gasification reactivity of coal chars by in-situ Raman spectroscopy. Fuel. 2020;270:117603.

[4] Yu G, Yu D, Liu F, Yu X, Han J, Wu J, et al. Different catalytic action of ion-exchanged calcium in steam and CO_2 gasification and its effects on the evolution of char structure and reactivity. Fuel. 2019;254:115609.

[5] Fang N, Li Z, Xie C, Liu S, Zeng L, Chen Z, et al. The application of fly ash gasification for purifying the raw syngas in an industrial-scale entrained flow gasifier. Energy. 2020;195:117069.

[6] Ding L, Zhou Z, Guo Q, Wang Y, Yu G. In situ analysis and mechanism study of char-ash/slag transition in pulverized coal gasification. Energ Fuel. 2015;29(6):3532–44.

[7] Janajreh I, Adeyemi I, Raza SS, Ghenai C. A review of recent developments and future prospects in gasification systems and their modeling. Renewable and Sustainable Energy Reviews. 2021;138:110505.
[8] Gao R, Huang B, Huang J, Xu J, Dai Z, Wang F. Process modelling of two-stage entrained-bed gasification composed of rapid pyrolysis and gasification processes. Fuel. 2020;262:116531.
[9] Li R, Xie M, Jin H, Guo L, Liu F. Effect of swirl on gasification characteristics in an entrained-flow coal gasifier. Int J Chem React Eng. 2020;18(3):20190203.
[10] Kobayashi N, Fujimori A, Tanaka M, Piao G, Itaya Y. Study of coal gasification using high ash fusion temperature coal in an entrained flow gasifier. J Chem Eng Jpn. 2015;48(1):22–8.
[11] Cao X, Kong L, Bai J, Ge Z, He C, Li H, et al. Effect of water vapor on coal ash slag viscosity under gasification condition. Fuel. 2019;237:18–27.
[12] He C, Bai J, Ilyushechkin A, Zhao H, Kong L, Li H, et al. Effect of chemical composition on the fusion behaviour of synthetic high-iron coal ash. Fuel. 2019;253:1465–72.
[13] Huang Z, Li Y, Lu D, Zhou Z, Wang Z, Zhou J, et al. Improvement of the Coal ash slagging tendency by coal washing and additive blending with mullite generation. Energ Fuel. 2013;27(4):2049–56.
[14] Li F, Yu B, Fan H, Guo M, Wang T, Huang J, et al. Investigation on regulation mechanism of red mud on the ash fusion characteristics of high ash-fusion-temperature coal. Fuel. 2019;257:116036.
[15] Wu C, Xin Y, Liu X, Li H, Jiao F. Synergistic effect of CaO and MgO addition on coal ash fusibility in a reducing atmosphere. Asia-Pac J Chem Eng. 2019;14:4.
[16] Zhang L, Wang J, Wei J, Bai Y, Song X, Xu G, et al. Synergistic effects of CaO and MgO on ash fusion characteristics in entrained-flow gasifier. Energ Fuel. 2021;35(1):425–32.
[17] Küçükbayrak S, Ersoy-Herigboyu A, Haykin-Açma H, Guner H, Urkan K. Investigation of the relation between chemical composition and ash fusion temperatures for soke Turkish lignites. Fuel Science&Technology International. 1993;11(9):1231–49.
[18] Saini MK, Srivastava PK. Effect of coal cleaning on ash composition and its fusion characteristics for a high-ash non-coking coal of India. Int J Coal Prep Util. 2017;37(1):1–11.
[19] Dai X, Bai J, Huang Q, Liu Z, Bai X, Lin C, et al. Coal ash fusion properties from molecular dynamics simulation: the role of calcium oxide. Fuel. 2018;216:760–7.
[20] Akiyama K, Pak H, Ueki Y, Yoshiie R, Naruse I. Effect of MgO addition to upgraded brown coal on ash-deposition behavior during combustion. Fuel. 2011;90(11):3230–6.
[21] Murakami K, Sato M, Tsubouchi N, Ohtsuka Y, Sugawara K. Steam gasification of Indonesian subbituminous coal with calcium carbonate as a catalyst raw material. Fuel Process Technol. 2015;129:91–7.
[22] Tsubouchi N, Mochizuki Y, Byambajav E, Hanaoka Y, Kikuchi T, Ohtsuka Y. Steam Gasification of Low-Rank Coals with Ion-Exchanged Sodium Catalysts Prepared Using Natural Soda Ash. Energ Fuel. 2017;31(3):2565–71.
[23] Śpiewak K, Czerski G, Porada S. Effect of K, Na and Ca-based catalysts on the steam gasification reactions of coal. Part II: Composition and amount of multi-component catalysts. Chem Eng Sci. 2021;229:116023.
[24] Mei Y, Wang Z, Bai J, He C, Li W, Liu T, et al. Mechanism of Ca additive acting as a deterrent to Na_2CO_3 deactivation during catalytic coal gasification. Energ Fuel. 2019;33(2):938–45.
[25] Gao M, Lv P, Yang Z, Bai Y, Li F, Xie K. Effects of Ca/Na compounds on coal gasification reactivity and char characteristics in H_2O/CO_2 mixtures. Fuel. 2017;206:107–16.
[26] Bai Y, Lv P, Li F, Song X, Su W, Yu G. Investigation into Ca/Na compounds catalyzed coal pyrolysis and char gasification with steam. Energ Convers Manage. 2019;184:172–9.
[27] Liu T, Yu Z, Mei Y, Feng R, Yang S, Wang Z, et al. Potassium migration and transformation during the deep reduction of oxygen carrier (OC) by char in coal-direct chemical looping hydrogen generation using potassium-modified Fe_2O_3/Al_2O_3 OC. Fuel. 2019;256:115883.
[28] Jing X, Wang Z, Zhang Q, Yu Z, Li C, Huang J, et al. Evaluation of CO_2 gasification reactivity of different coal rank chars by physicochemical properties. Energ Fuel. 2013;27(12):7287–93.
[29] Goyal A, Zabransky RF, Rehmat A. Gasification kinetics of Western Kentucky bituminous coal char. Ind Eng Chem Res. 1989;28(12):1767–78.
[30] Dutta S, Wen CY, Belt RJ. Reactivity of coal and char 1 in carbon dioxide atmosphere. Industrial Eng Chem Process Des Development. 1977;16(1):20–30.
[31] Tran K, Bui H, Luengnaruemitchai A, Wang L, Skreiberg Ø. Isothermal and non-isothermal kinetic study on CO_2 gasification of torrefied forest residues. Biomass and Bioenergy. 2016;91:175–85.
[32] Lahijani P, Zainal ZA, Mohamed AR, Mohammadi M. CO_2 gasification reactivity of biomass char: Catalytic influence of alkali, alkaline earth and transition metal salts. Bioresource Technol. 2013;144:288–95.
[33] Shankar K, Evans JW. A structural model for gas-solid reactions with a moving boundary. Chem Eng Sci. 1970;25:1091–107.
[34] Wang F, Zeng X, Wang Y, Yu J, Xu G. Characterization of coal char gasification with steam in a micro-fluidized bed reaction analyzer. Fuel Process Technol. 2016;141:2–8.
[35] Levenspiel O. Chemical reaction engineering. New York: Wiley; 1975.
[36] Bai Y, Yang X, Li F, Wang J, Song X, Yao M, et al. Calcium species evolution mechanism during coal pyrolysis and char gasification in H_2O/CO_2. J Energy Inst. 2020;93(4):1324–31.
[37] Yu G, Yu D, Liu F, Han J, Yu X, Wu J, et al. Different impacts of magnesium on the catalytic activity of exchangeable calcium in coal gasification with CO_2 and steam. Fuel. 2020;266:117050.

Appendix

Table A1: Actual concentrations of flux in partial prepared samples

Flux	Theoretical concentration (%)			
	1	2	5	10
Na_2CO_3	1.05	2.09	4.93	10.09
NaCl	1.03	1.95	5.10	10.11
Na_2SiO_3	0.98	1.92	5.09	9.93
Na_2SO_4	0.99	1.96	4.97	10.20
$CaCO_3$	1.02	2.07	5.11	10.03
CaO	1.04	2.04	5.12	10.31
$CaCl_2$	1.06	1.98	5.09	9.88
$CaSO_4$	1.05	2.10	4.97	9.93
$CaSiO_3$	0.97	2.03	4.99	10.18

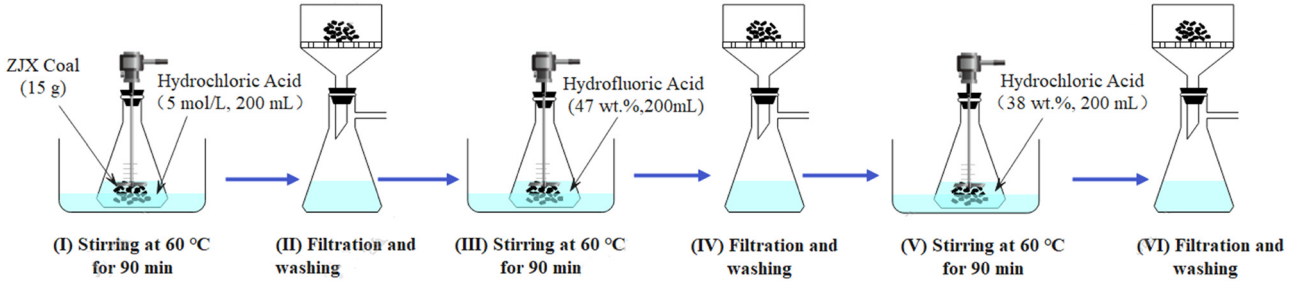

Figure A1: Detailed procedure of acid deashing process.